Electronic Supplementary Information

Weak intermolecular interactions promote blue luminescence of protonated 2,2'-dipyridylamine salts

Alexander N. Chernyshev,[a,b] Dmitry Morozov,[a,c] Jarkko Mutanen,[d] Vadim Yu. Kukushkin,[b] Gerrit Groenhof,*[,a,c] and Matti Haukka*[,a]

[a]*Department of Chemistry, University of Jyväskylä, P.O. Box 35, FI-40014 Jyväskylä, Finland*
[b]*Department of Chemistry, Saint Petersburg State University, 198504 Stary Petergof, Russian Federation*
[c]*Nanoscience Center, Univeristy of Jyväskylä, P.O. Box 35, FI-40014 Jyväskylä, Finlan*
[d]*Institute of Photonics, University of Eastern, Finland, P.O.Box 111, FI-80101, Joensuu, Finland*

TABLE OF CONTENTS

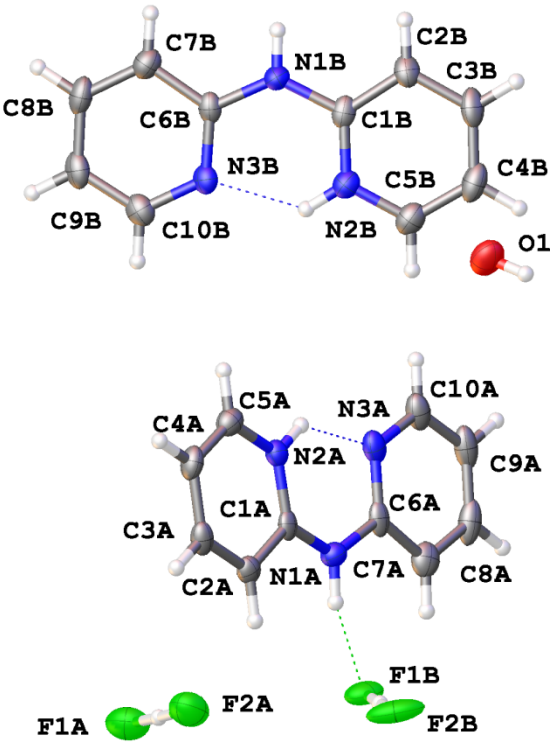

Figure S1. Crystal structure of **1** at 100 K with 50% thermal ellipsoids and labeling scheme.

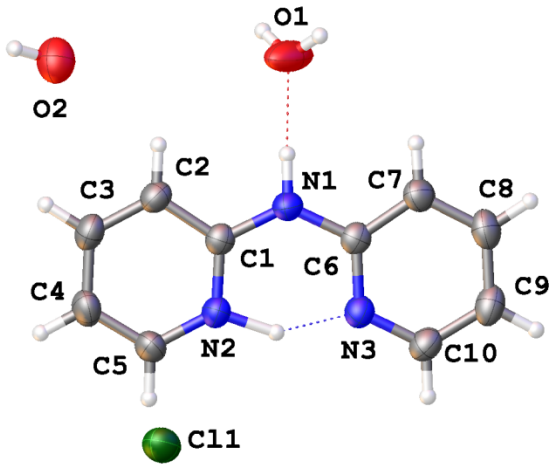

Figure S2. Crystal structure of **2** at 290 K with 50% thermal ellipsoids and labeling scheme.

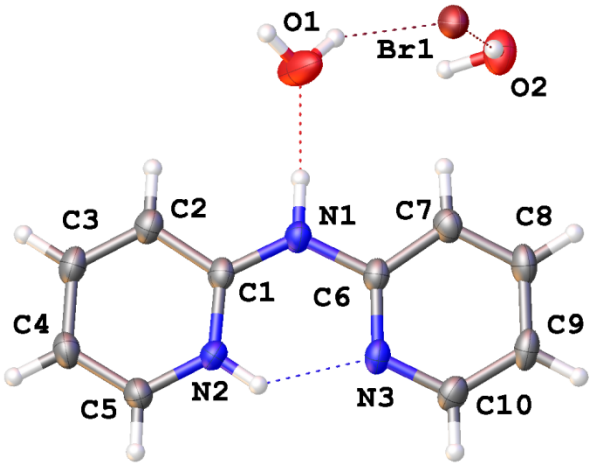

Figure S3. Crystal structure of **3** at 170 K with 50% thermal ellipsoids and labeling scheme.

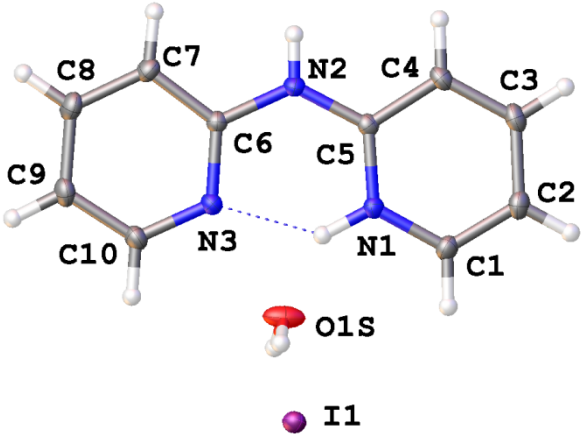

Figure S4. Crystal structure of **4a** at 100 K with 50% thermal ellipsoids and labeling scheme.

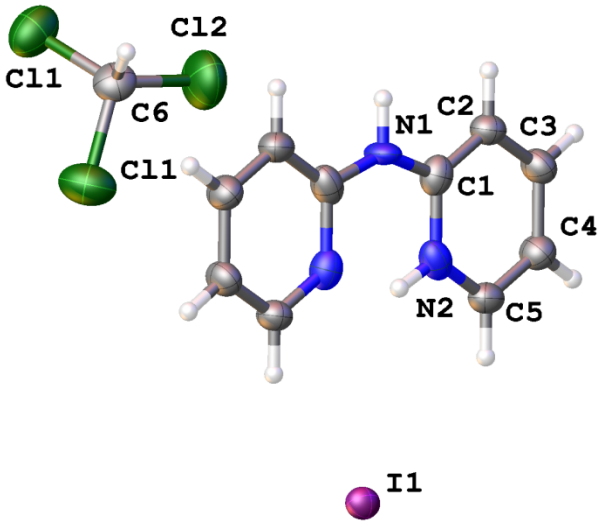

Figure S5. Crystal structure of **4b** at 170 K with 50% thermal ellipsoids and labeling scheme. Only one component of the disordered system is shown.

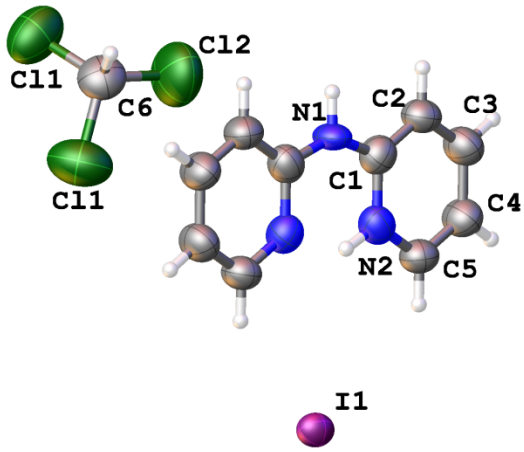

Figure S6. Crystal structure of **4b** at 290 K with 50% thermal ellipsoids and labeling scheme. Only one component of the disordered system is shown.

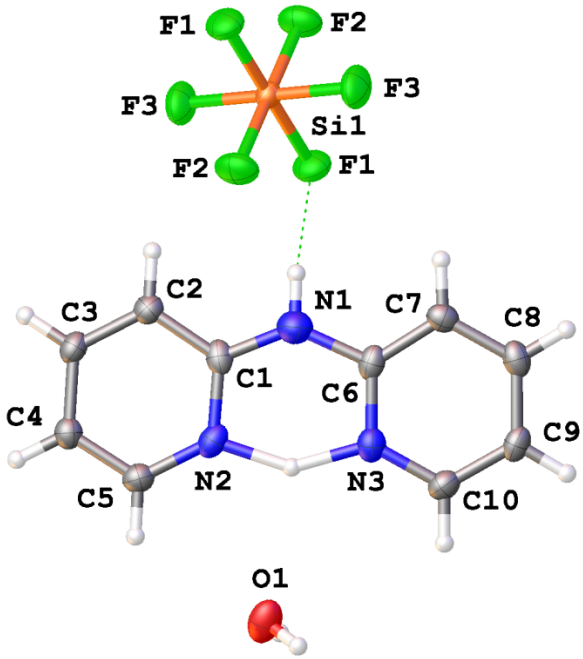

Figure S7. Crystal structure of **5** at 170 K with 50% thermal ellipsoids and labeling scheme.

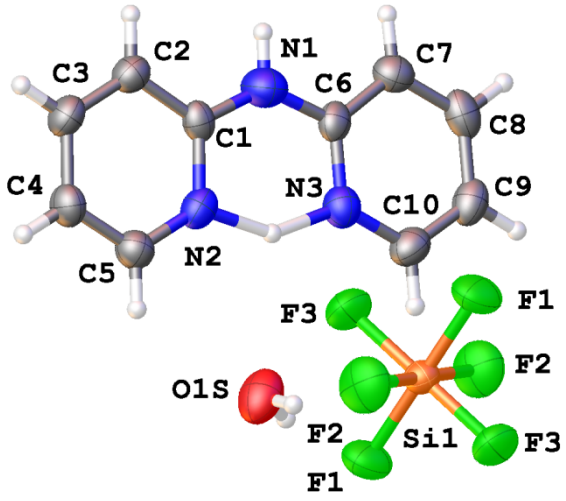

Figure S8. Crystal structure of **5** at 290 K with 50% thermal ellipsoids and labeling scheme.

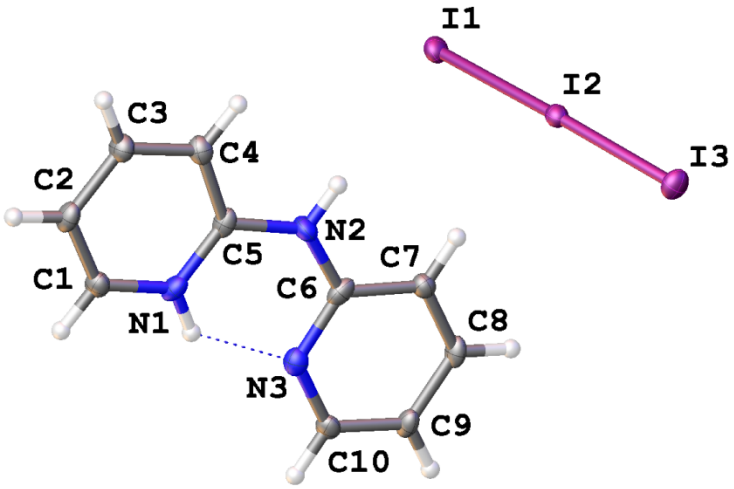

Figure S9. Crystal structure of **6** at 100 K with 50% thermal ellipsoids and labeling scheme.

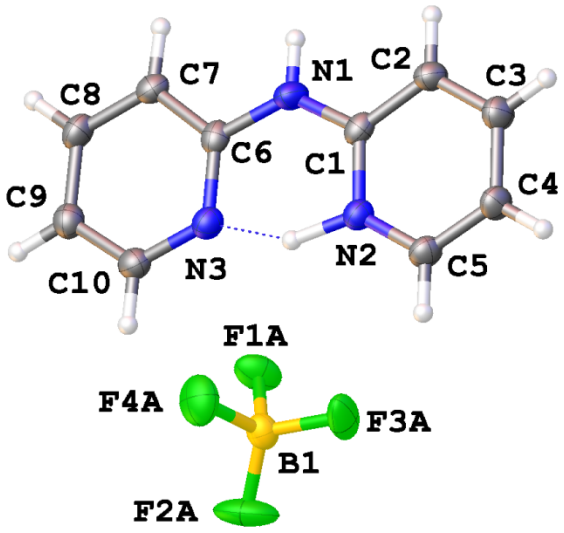

Figure S10. Crystal structure of **8** at 100 K with 50% thermal ellipsoids and labeling scheme. Fluorine atoms are disordered over two sites and only one site is shown.

Table S1. Crystal data.

	1 at 100 K	**2 at 290 K**	**3 at 170 K**	**4a at 100 K**	**4b at 170 K**	**4b at 290 K**	**5 at 170 K**	**5 at 290**
empirical formula	$C_{20}H_{24}F_4N_6O$	$C_{10}H_{14}ClN_3O_2$	$C_{10}H_{14}BrN_3O_2$	$C_{10}H_{12}IN_3O$	$C_{11}H_{11}Cl_3IN_3$	$C_{11}H_{11}Cl_3IN_3$	$C_{10}H_{12}F_3N_3OSi_{0.5}$	$C_{10}H_{12}F_3N_3OSi_{0.5}$
fw	440.45	243.69	288.15	317.13	418.48	418.48	261.27	261.27
temp (K)	100(2)	290(2)	170(2)	100(2)	170(2)	290(2)	170(2)	290(2)
λ(Å)	1.54184	0.71073	0.71073	0.71073	0.71073	0.71073	0.71073	0.71073
cryst syst	Orthorhombic	Monoclinic	Monoclinic	Triclinic	Orthorhombic	Orthorhombic	Triclinic	Triclinic
space group	Pbc21	Cc	Cc	P $\bar{1}$	Pnma	Pnma	P $\bar{1}$	P $\bar{1}$
a (Å)	13.9450(2)	9.6007(2)	9.5861(2)	7.3741(5)	10.55750(13)	10.65379(12)	7.1165(5)	7.1604(10)
b (Å)	7.63438(9)	15.8730(3)	16.1448(3)	8.9009(6)	14.04189(18)	14.07388(14)	9.0759(7)	9.0853(5)
c (Å)	19.5974(3)	7.97687(18)	8.18095(16)	9.5009(6)	10.38870(13)	10.48437(10)	9.8120(8)	9.8694(6)
α (deg)	90	90	90	104.349(2)	90	90	117.118(8)	117.066(2)
β (deg)	90	105.107(2)	107.024(2)	108.232(3)	90	90	99.869(6)	100.294(3)
γ (deg)	90	90	90	90.833(3)	90	90	98.207(6)	98.373(3)
V (Å^3)	2086.36(5)	1173.59(5)	1210.65(4)	570.94(7)	1540.10(3)	1572.03(3)	537.80(8)	543.33(9)
Z	4	4	4	2	4	4	2	2
ρ_{calc} (Mg/m3)	1.402	1.379	1.581	1.845	1.805	1.768	1.613	1.597
μ(Mo Kα) (mm^{-1})	0.987	0.315	3.386	2.783	2.586	2.533	0.195	0.193
No. reflns.	6831	9503	9275	23341	15604	34119	4321	9282
Unique reflns.	2475	3110	2997	7046	2344	2276	2227	2478
GOOF (F^2)	1.031	1.117	1.109	1.132	1.056	0.945	1.073	1.043
R_{int}	0.0168	0.0188	0.0398	0.0315	0.0212	0.0207	0.0089	0.0370
R1[a] ($I \geq 2\sigma$)	0.0425	0.0348	0.0384	0.0194	0.0230	0.0283	0.0666	0.0712
wR2[b] ($I \geq 2\sigma$)	0.1189	0.0976	0.0936	0.0510	0.0489	0.0823	0.1911	0.2060

Table S1. Extension. Crystal Data.

	6 at 100 K	**8 at 100 K**
empirical formula	$C_{10}H_{10}I_3N_3$	$C_{10}H_{10}BF_4N_3$
fw	552.91	259.02
temp (K)	100(2)	100(2)
λ(Å)	0.71073	0.71073
cryst syst	Triclinic	Monoclinic
space group	P $\bar{1}$	P 21/c
a (Å)	8.9204(8)	8.2733(5)
b (Å)	9.0608(7)	15.9517(10)
c (Å)	9.6164(8)	8.6360(5)
α (deg)	82.098(3)	90
β (deg)	87.091(3)	103.447(3)
γ (deg)	65.791(3)	90
V (Å^3)	702.15(10)	1108.48(12)
Z	2	4
ρ_{calc} (Mg/m3)	2.615	1.552
μ(Mo Kα) (mm^{-1})	6.657	0.142
No. reflns.	13070	10637
Unique reflns.	3605	2542
GOOF (F^2)	1.142	1.082
R_{int}	0.0345	0.0390
R1[a] ($I \geq 2\sigma$)	0.0285	0.0469
wR2[b] ($I \geq 2\sigma$)	0.0848	0.1210

[a] $R1 = \Sigma||F_o| - |F_c||/\Sigma|F_o|$. [b] $wR2 = [\Sigma[w(F_o^2 - F_c^2)^2]/ \Sigma[w(F_o^2)^2]]^{1/2}$.

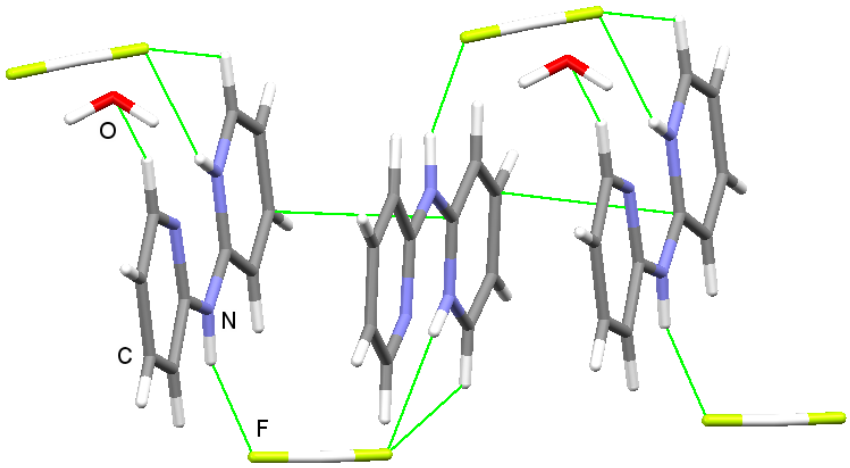

Figure S11. The π-stacking interactions, supported by hydrogen bonds in (dpaH)[HF_2]·0.5H_2O (**1**).

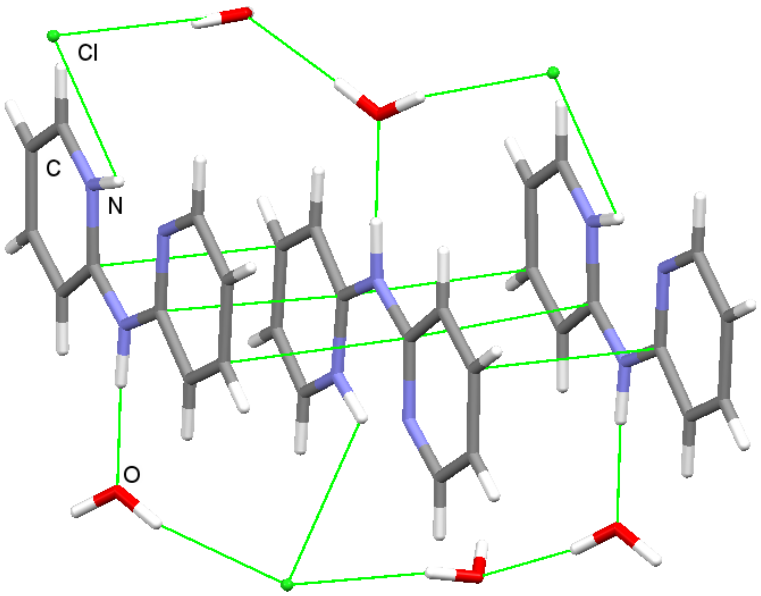

Figure S12. The π-stacking interactions, supported by hydrogen bonds in (dpaH)Cl·2H_2O (**2**).

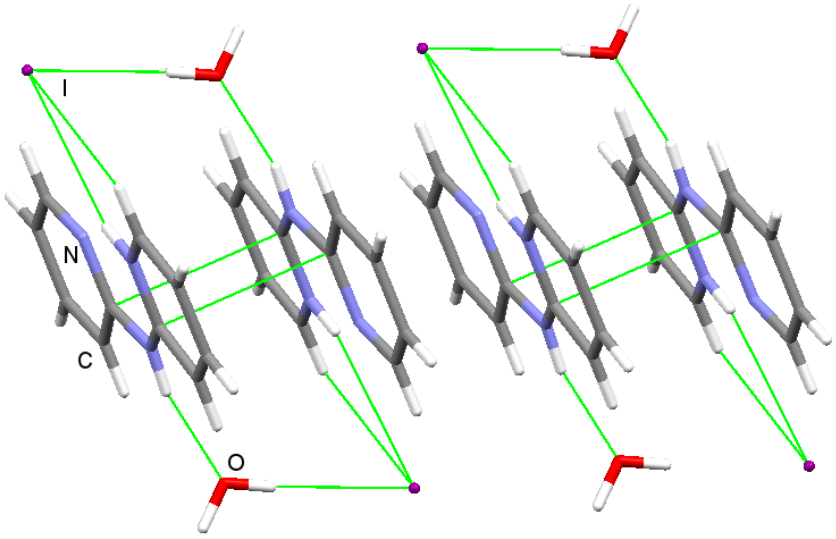

Figure S13. The π-stacking interactions, supported by hydrogen bonds in (dpaH)I·H_2O (**4a**).

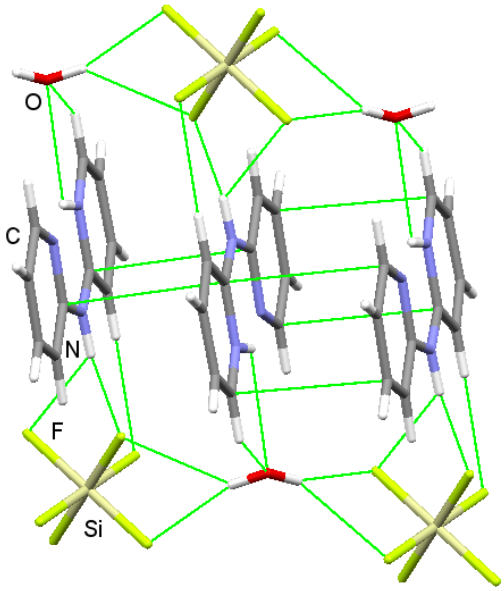

Figure S14. The π-stacking interactions, supported by hydrogen bonds in $(dpaH)_2[SiF_6]\cdot H_2O$ (**5**).

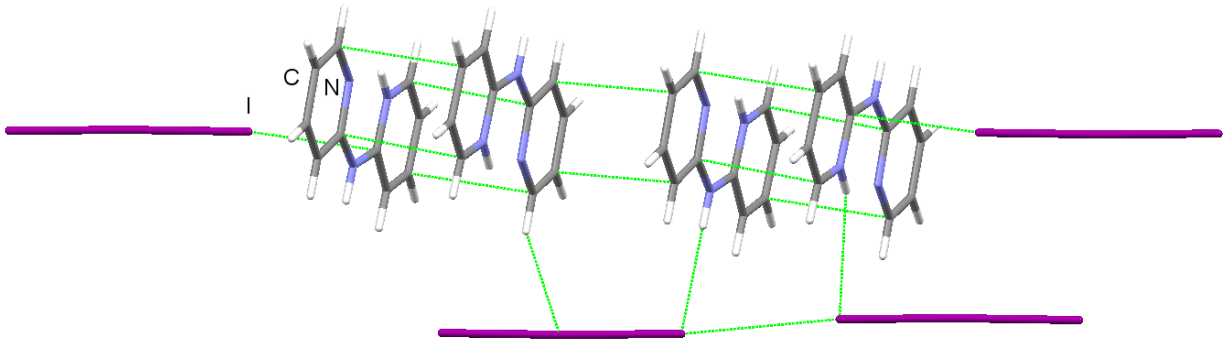

Figure S15. The π-stacking interactions, supported by hydrogen bonds in $(dpaH)[I_3]$ (**6**).

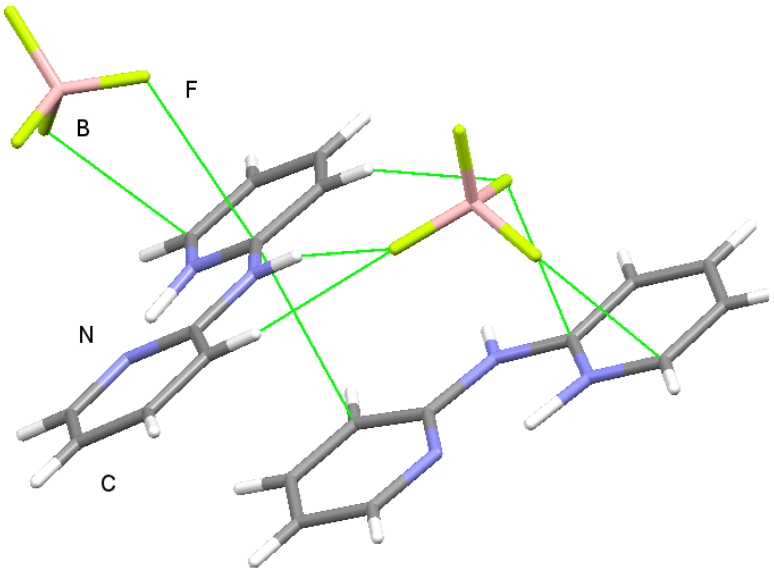

Figure S16. The π-stacking interactions, supported by hydrogen bonds in (dpaH)[BF_4] (**8**).

Table S2. Absorption maxima of the compounds **1**–**5**, **7** and **8** in MeOH and CHCl3.

Substance	Methanol solution			Chloroform solution	
1	264	311	259	292-299, bad resolved peaks	330
2	264	311	259	289-297, bad resolved peaks	330
3	264	311	258	287-296, bad resolved peaks	329
4	264	311	259	286-295, bad resolved peaks	328
5	264	311	258	286-296, bad resolved peaks	327
7	264	311	259	288-296, bad resolved peaks	326
8	264	311	256	285-294, bad resolved peaks	327

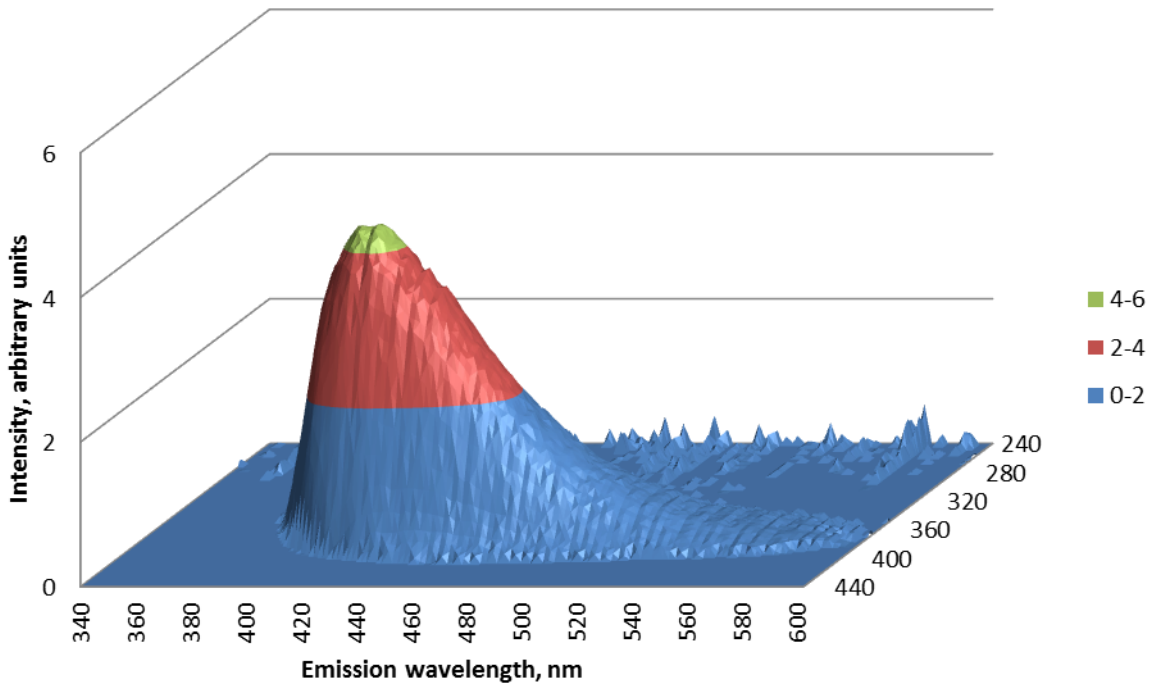

Figure S17. Excitation-emission matrix of solid (dpaH)[HF_2]•0.5H_2O (**1**).

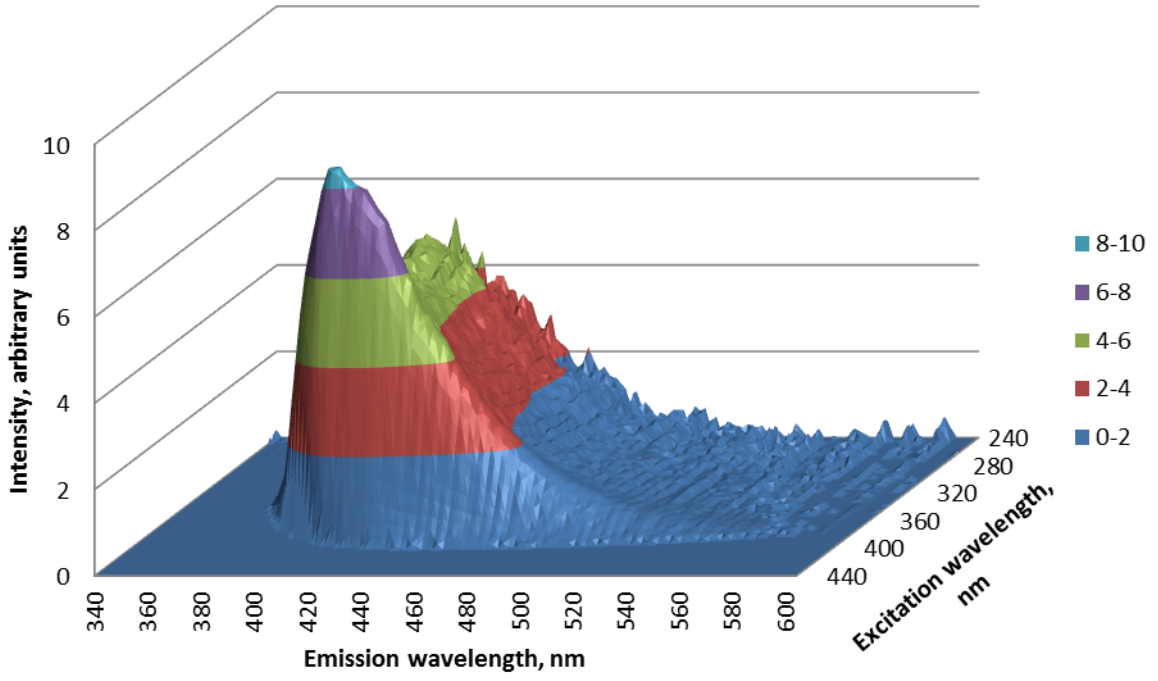

Figure S18. Excitation-emission matrix of solid (dpaH)Cl•2H_2O (**2**).

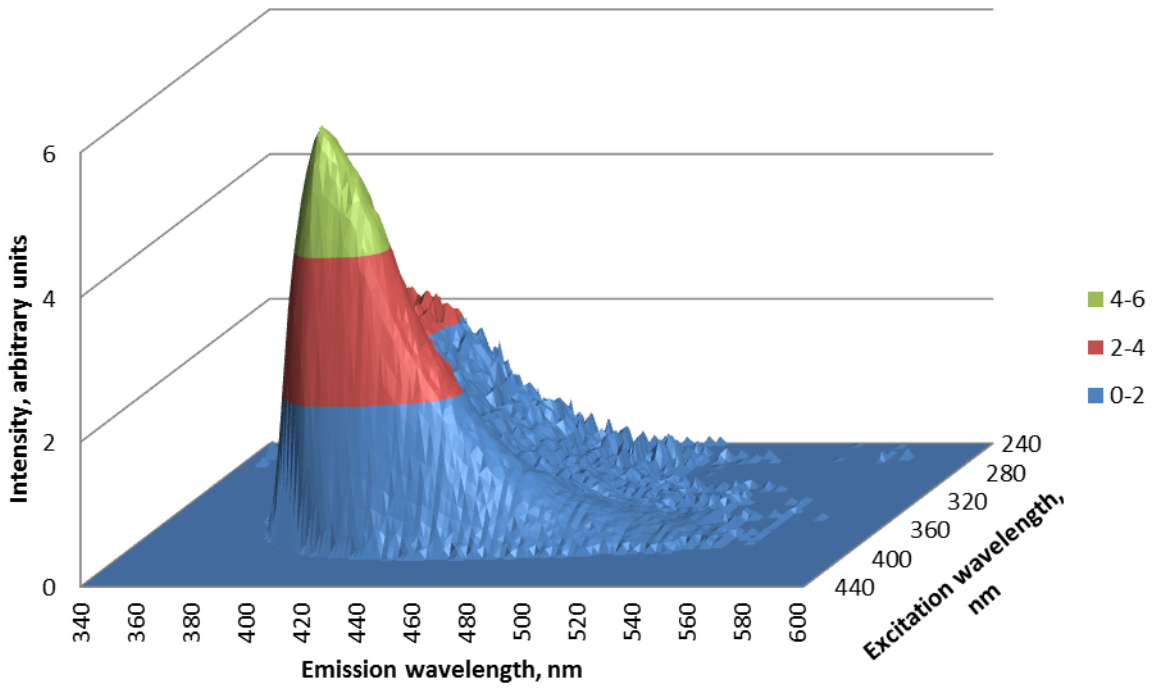

Figure S19. Excitation-emission matrix of solid (dpaH)Br•$2H_2O$ (**3**).

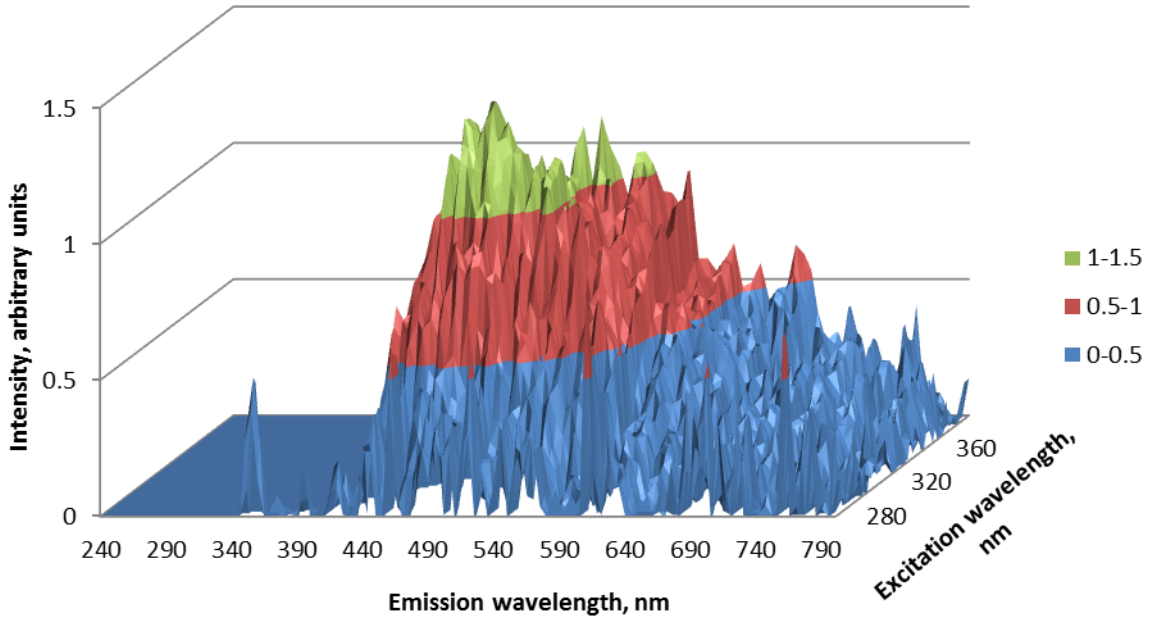

Figure S20. Excitation-emission matrix of solid (dpaH)I•$CHCl_3$ (**4b**). Due to very low emission intensity the quality of the spectrum is poor.

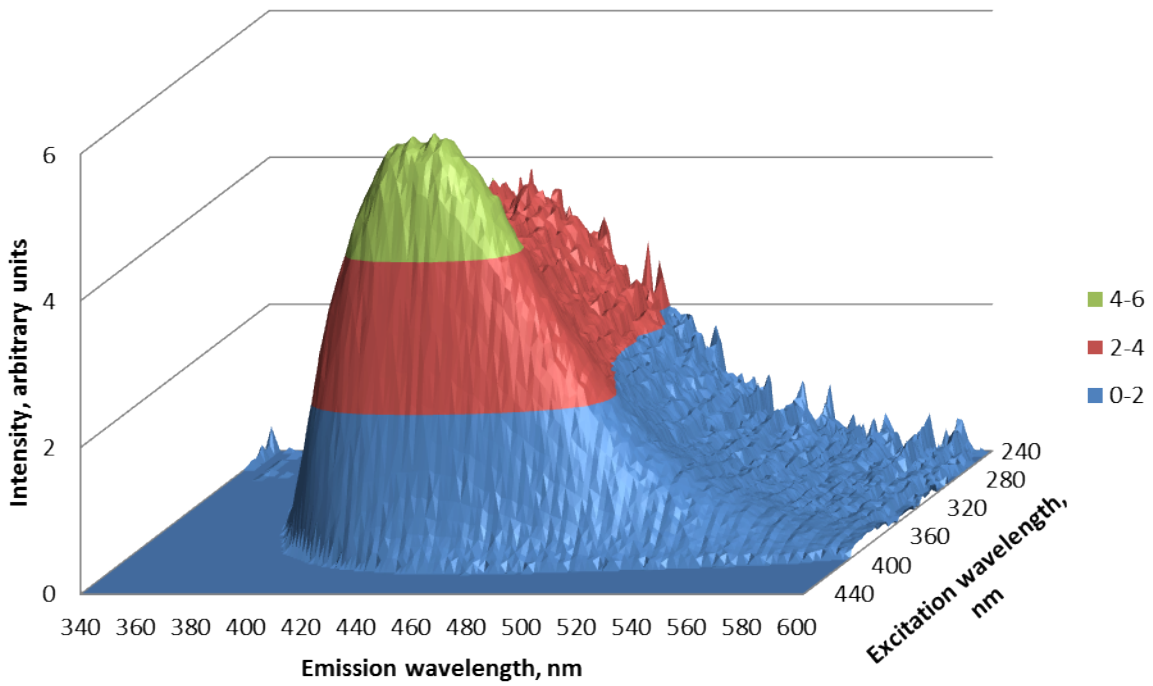

Figure S21. Excitation-emission matrix of solid $(dpaH)_2[SiF_6]\bullet H_2O$ (**5**).

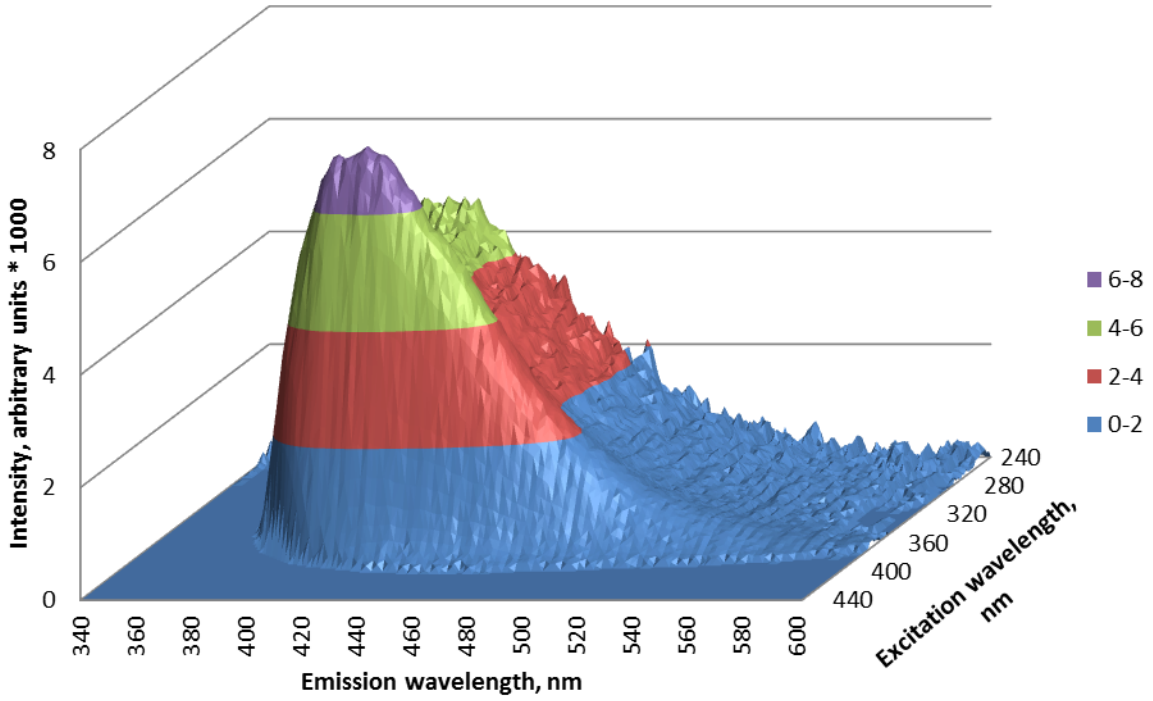

Figure S22. Excitation-emission matrix of solid $(dpaH)_2[SbF_6]$ (**7**).

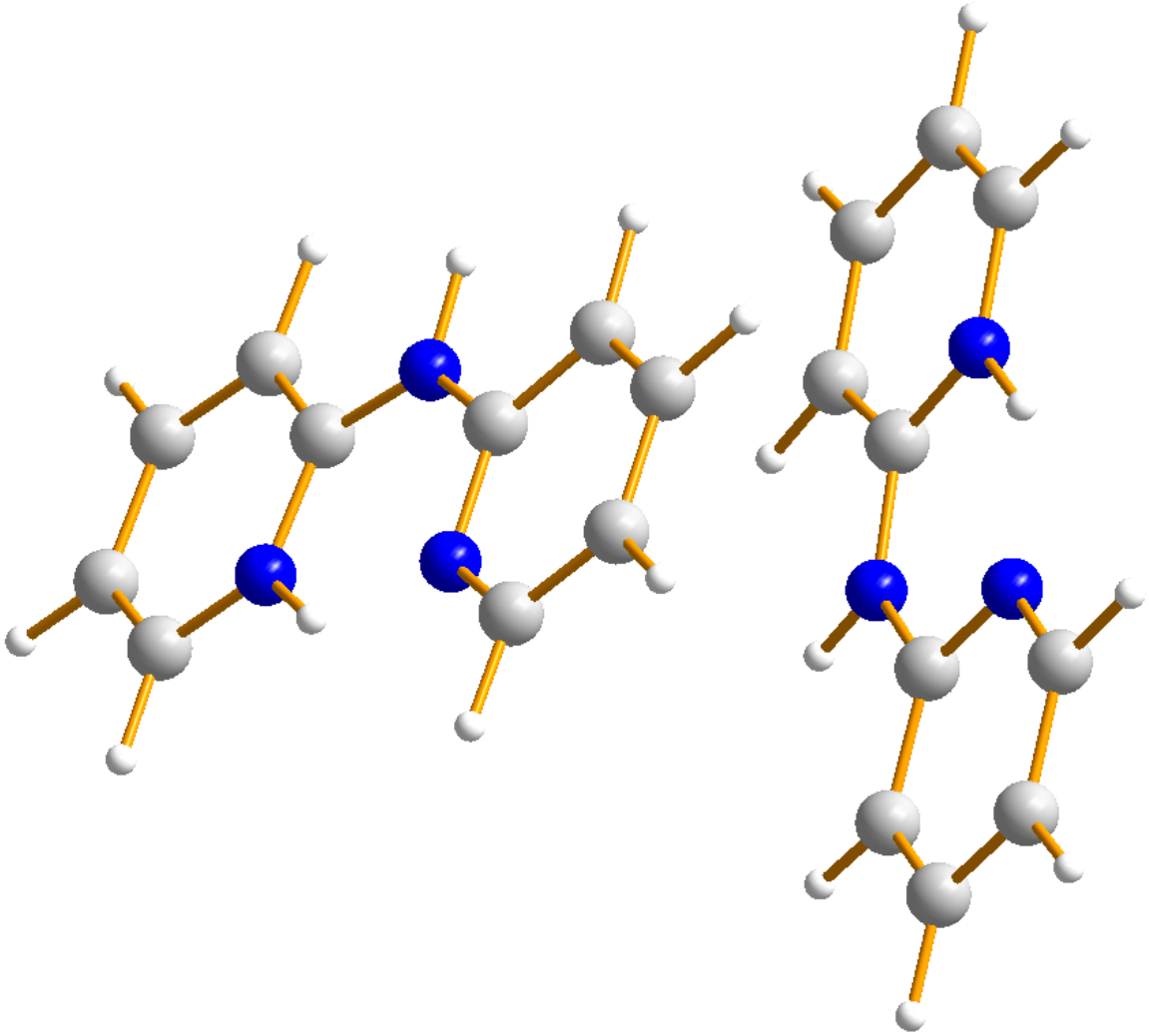

Figure S23. Geometry of dpa cation dimer from crystal **8**.

Table S3. Calculated vertical excitation energies of the stacked dpa dimmer from structure **8**.

Transition	E, eV	E, nm
S0->S1	3.71	334
S0->S2	3.99	310
S0->S3	4.45	278
S0->S4	4.79	258

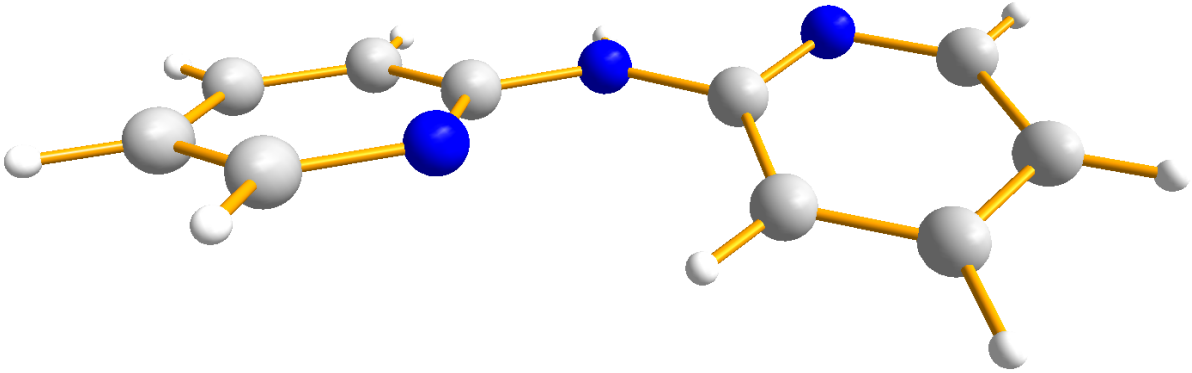

Figure S24. Geometry of the neutral dpa on ground state.

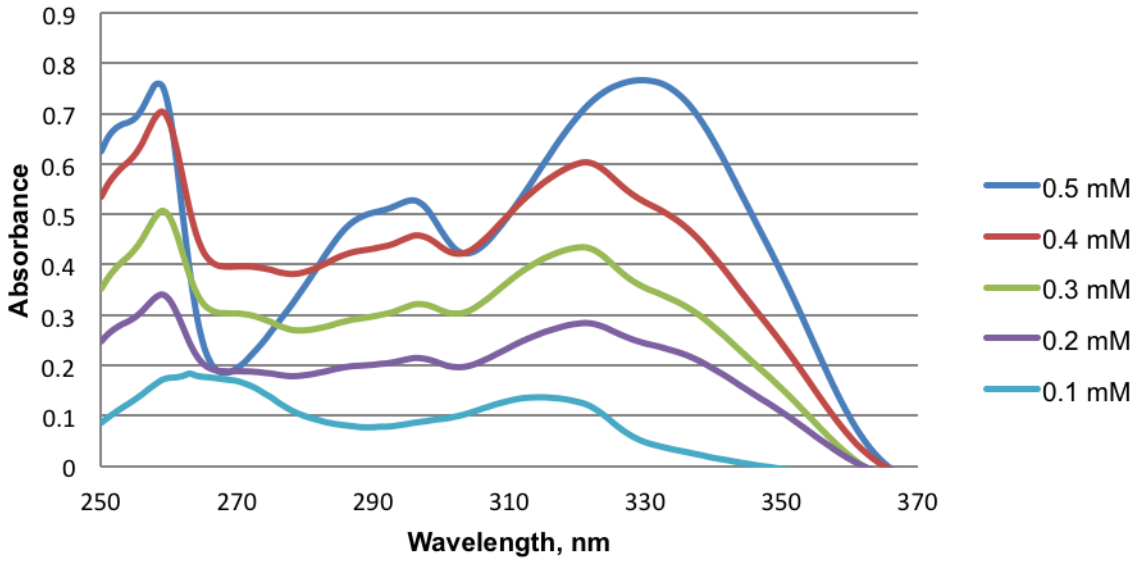

Figure S25. Concentration dependent absorption spectra of chloroform solutions of **3**.